NIH Public Access
Author Manuscript
Biochemistry. Author manuscript; available in PMC 2012 August 23.

Published in final edited form as:
Biochemistry. 2011 August 23; 50(33): 7157–7167. doi:10.1021/bi200435n.

Pro-inflammatory exoprotein characterization of toxic shock syndrome *Staphylococcus aureus*†

Ying-Chi Lin[‡], **Michele J. Anderson**[‡], **Petra L. Kohler**[§], **Kristi L. Strandberg**[§], **Michael E. Olson**[†], **Alexander R. Horswill**[†], **Patrick M. Schlievert**[§], and **Marnie L. Peterson**[‡,§,*]

[‡]Department of Experimental and Clinical Pharmacology, College of Pharmacy, University of Minnesota, Minneapolis, Minnesota 55455

[§]Department of Microbiology, Medical School, University of Minnesota, Minneapolis, Minnesota 55455

[†]Department of Microbiology, University of Iowa, Iowa City, IA 52242

Abstract

Pulsed-field gel electrophoresis (PFGE) clonal type USA200 is the most widely disseminated *Staphylococcus aureus* colonizer of the nose and is a major cause of toxic shock syndrome (TSS). Exoproteins derived from these organisms have been suggested to contribute to their colonization and causation of human diseases, but have not been well-characterized. Two representative *S. aureus* USA200 isolates, MNPE (α-toxin positive) and CDC587 (α-toxin mutant), isolated from pulmonary post-influenza TSS and menstrual vaginal TSS, respectively, were evaluated. Biochemical, immunobiological and cell-based assays, including mass spectrometry, were used to identify key exoproteins derived from the strains that are responsible for pro-inflammatory and cytotoxic activity on human vaginal epithelial cells. Exoproteins associated with virulence were produced by both strains, and cytolysins (α-toxin and γ-toxin), superantigens, and proteases were identified as the major exoproteins, which caused epithelial cell inflammation and cytotoxicity. Exoprotein fractions from MNPE were more pro-inflammatory and cytotoxic than those from CDC587 due to high concentrations of α-toxin. CDC587 produced a small amount of α-toxin, despite the presence of a stop codon (TAG) at codon 113. Additional exotoxin identification studies of USA200 strain [*S. aureus* MN8 (α-toxin mutant)] confirmed that MN8 also produced low levels of α-toxin despite the same stop codon. The differences observed in virulence factor profiles of two USA200 strains provide insight into environmental factors that select for specific virulence factors. Cytolysins, superantigens, and proteases were identified as potential targets, where toxin neutralization may prevent or diminish epithelial damage associated with *S. aureus*.

Staphylococcus aureus is the most common cause of ventilator-associated pneumonia, surgical site infections, and catheter-associated bloodstream infections in the healthcare setting as well as a frequent cause of skin and pulmonary infections in the community (1). About 30% of people are colonized by *S. aureus* in their nose and on their skin (2). *S. aureus* carriers have three-fold higher risk for *S. aureus* infections than non-carriers, with a majority (80%) of the infections being caused by the patient's own endogenous strains present on

[†]NIH: National Institute of Allergy and Infectious Diseases AI-74283(PMS), AI-73366 (MLP), AI-078921 (ARH) and AI-07511 (MEO), Powell Center for Women's Health and University of Minnesota Academic Heath Center Office of the Vice President (MLP), U54-AI57153 Great Lakes Regional Center of Excellence in Biodefense and Emerging Infectious Diseases (PMS), and 3M Non-tenured unrestricted faculty research award (MLP)

[*]Corresponding author: Department of Experimental and Clinical Pharmacology, College of Pharmacy, University of Minnesota, 4-212 McGuire Translational Research Facility, 2001 6th St. S.E., Minneapolis, MN 55455, Phone: 612-626-4388, Fax: 612-626-9985, peter377@umn.edu.

NIH-PA Author Manuscript
NIH-PA Author Manuscript
NIH-PA Author Manuscript

NIH-PA Author Manuscript

NIH-PA Author Manuscript

NIH-PA Author Manuscript

mucosal surfaces and skin (3). Pulsed-field gel electrophoresis (PFGE) clonal type USA200 is the most widely disseminated methicillin-sensitive *S. aureus* (MSSA) colonizer of the nose, a cause of invasive nosocomial (healthcare-associated) infections, and the major cause of staphylococcal toxic shock syndrome (TSS) (4–5).

S. aureus initiates illnesses at mucosal surfaces or skin where numerous exotoxins and other secreted virulence factors participate. *S. aureus* exoproteins, including the superantigens staphylococcal enterotoxins (SEs), staphylococcal enterotoxin-like (SEl) proteins, and TSS toxin-1 (TSST-1), and cytolysins (hemolysins and leukocidins), have been reported to play important roles in *S. aureus* diseases. Staphylococcal superantigens, which are named by their ability to induce massive production of cytokines by a non-antigen specific cross-linkage of T-cells and major histocompatibility complex (MHC) class II molecules on antigen-presenting cells, mediate severe diseases such as TSS, an acute onset systemic disease with multiple organ involvement. TSS has been associated with vaginal colonization of *S. aureus* that produce superantigens, especially TSST-1, during menstruation, or as a complication of influenza with secondary *S. aureus* infections. Approximately 25% of nasal isolates and 5% of vaginal mucosal isolates possess, *tst*, the gene that encodes TSST-1, and more than 90% of these isolates are USA200 (4, 6).

In addition to superantigens, the cytolysins, notably α-toxin (α-hemolysin; encoded by the gene *hla*), have also been shown to play important roles in *S. aureus* illnesses. Alpha-toxin was recently determined to cause significant lung tissue damage in a murine staphylococcal pneumonia model, a system that does not assess superantigen effects (7). Alpha-toxin is highly pro-inflammatory and cytolytic to various mammalian cells, including erythrocytes, monocytes, endothelial cells, and epithelial cells (8). Our research group has previously demonstrated that α-toxin facilitates TSST-1 penetration of porcine vaginal mucosa by induction of pro-inflammatory responses and disruption within the mucosal barrier (9). However, 75% of menstrual TSS vaginal isolates are considered unable to produce α-toxin due to a defective α-toxin gene, *hla*$^{-}$, which has a nonsense point mutation (CAG [Gln] to TAG [stop codon]) at codon 113 (10). These menstrual TSS strains were also noted to produce lower quantities of lipase, nuclease, and overall hemolysins than isolates from skin (11).

Proteomic approaches have been used to facilitate our understanding of *S. aureus* pathogenesis to identify potential targets for therapeutic development. However, most proteomic studies to date focused on MRSA strains associated with community-associated infections, USA300 and USA400, or laboratory strains (12–13). Although important, these studies mainly focused on identifying proteins differentially expressed by strains, but provided limited information about the relative biological contribution of these exoproteins to *S. aureus* pathogenesis. Given the prior knowledge that inflammation and direct disruption of the mucosa facilitates superantigen penetration through mucosal surfaces, we designed this study, combining biological testing and proteomic approaches to identify key exoproteins produced by *S. aureus* that are responsible for inflammation and cytotoxicity to epithelial cells. Two representative *S. aureus* USA200 isolates, which cause distinguishable types of TSS, menstrual TSS and post-influenza pulmonary TSS, were selected for characterization of their exotoxin profiles, which likely contributed to their respective diseases. Global analyses via high-level purification [reverse phase high performance liquid chromatography (rHPLC)] combined with mass spectrometry determined that 9 and 24 *S. aureus* exoproteins associated with staphylococcal pathogenesis were detected from the post-influenza pulmonary TSS isolate (MNPE) and menstrual vaginal TSS isolate (CDC587), respectively. Of those, cytolysins, superantigens, and staphopain A account for most pro-inflammatory and cytotoxic activities to epithelial cells. We also provide evidence that the menstrual TSS isolate (CDC587) produces a small amount of α-toxin, despite the

NIH-PA Author Manuscript

NIH-PA Author Manuscript

NIH-PA Author Manuscript

presence of a stop codon (TAG) at codon 113. Additional exotoxin identification studies of USA200 strain [*S. aureus* MN8 (α-toxin mutant)] confirmed that MN8 also produced low levels of α-toxin despite containing the same stop codon. In addition, the differences in exoprotein profiles between the two *S. aureus* isolates (MNPE and CDC587) may have implications for bacterial virulence factor selection via their respective host niches of skin versus vaginal mucosa.

EXPERIMENTAL PROCEDURES (MATERIALS AND METHODS)

Bacteria

USA200 isolates, MNPE and CDC587, were used extensively in this study. Both strains are methicillin-susceptible *S. aureus* (MSSA). *S. aureus* MNPE was isolated from a post-influenza pulmonary TSS case in 1987, most likely originating from a skin source (14), and CDC587 is a typical menstrual vaginal TSS strain isolated from a patient in 1980 (15). The strains were maintained in Dr. Schlievert laboratory (lyophilized; low passage). Polymerase chain reaction (PCR) (16) revealed that MNPE carries the superantigen genes for TSST-1, SEA, SEC, SEl-G, SEI, SEl-K, SEl-L, SEl-M, SEl-N, SEl-O, and SEl-P, while CDC587 also carries the genes for SEA, SEC, SEl-G, SEI, SEl-K, SEl-L, SEl-M, SEl-N, SEl-O, and SEl-P. The major difference between the two strains is that CDC587 possesses a defective α-toxin gene (*hla*$^{-}$), a nonsense point mutation (CAG [Gln] to TAG [stop codon]) at codon 113, while MNPE carries a wild-type α-toxin (*hla*$^{+}$). Both strains have the γ-toxin gene (*hlg*$^{+}$). An additional menstrual vaginal TSS MSSA USA200 isolate, MN8, which also carries *hla* with the (CAG [Gln] to TAG [stop codon]) at codon 113 (*hla*$^{-}$), was used to confirm α-toxin production in some experiments.

Porcine *ex vivo* vaginal mucosal experiments

Porcine vaginal mucosal tissue was used in initial experiments of *S. aureus* toxicity, as it was previously reported to be histologically and structurally similar to human vaginal mucosa (17). This porcine *ex vivo* vaginal mucosal infection model was developed by our laboratory and described previously (18). Briefly, porcine vaginal tissue samples with uniform size were prepared from fresh porcine vaginal mucosa using 5 mm tissue biopsy punches. The basal side of the samples were supplemented with 10% FCS and antibiotic-free RPMI 1640. The mucosal surface of each was challenged with 10^7 colony-forming units (CFU) of bacteria suspended in antibiotic-free RPMI 1640. At 24 h, samples were fixed in 10% phosphate-buffered formalin for histological examination by hemotoxylin and eosin staining.

Exoprotein preparation and separation

Bacteria were grown overnight in beef heart medium supplemented with 1% glucose-phosphate buffer (2 liters, made in-house) in ambient air with aeration at 37 °C, which favors exotoxin production (19). Bacterial cells were removed by centrifugation (3,220 g, 10 min at 4 °C). Proteins in the supernates were precipitated overnight at room temperature by ammonium sulfate (80% final concentration). Precipitates were collected by centrifugation (3,220 g, 15 min at 4 °C) and resolubilized in sterile distilled water (SDW). Excess salts and proteins with molecular weights smaller than 14 kDa were removed by dialyzing samples against SDW. Insoluble materials were removed by centrifugation at 8000 g for 30 min. Samples (75–100 ml) were mixed with Sephadex G75 (pre-washed with ethanol, Sigma, St. Louis, MO) to generate a thick gel. Thin-layer isoelectric focusing (IEF) in pH gradients of 3–10 were used to separate proteins into 15 fractions. The IEF were run at 1000 V, 8 W, and 20 mA for 24 h. The fractions were eluted with water and pH of the fractions was measured following IEF separation. The samples were dialyzed against SDW for 3 days to remove ampholyte buffers prior to lyophilization. The lyophilized protein fractions were dissolved

NIH-PA Author Manuscript

NIH-PA Author Manuscript

NIH-PA Author Manuscript

in SDW and the protein concentrations were estimated by the Bradford method (20). A secondary IEF (pH gradient 7–9) was applied to further separate fractions 12–15 from the primary IEF. IEF of the MNPE fractions was separated into 15 fractions, while CDC587 IEF was separated into 12 fractions according to the visual protein patterns observed in the gel matrix (fractions 4–15). Protein compositions of the fractionated proteins (about 250 ng loaded) were determined by 12% sodium dodecyl sulfate polyacrylamide gel electrophoresis (SDS-PAGE) and silver-staining.

High performance liquid chromatography

According to the protein patterns on the SDS gels, select fractions were further resolved by reverse phase high performance liquid chromatography (rHPLC). The rHPLC was done on a Hewlett-Packard AminoQuant 1090L HPLC system with an Agilent Zorbax SB-CN (4.6 × 150 mm; 5 μm) column. Solvent A was 0.1% (v/v) trifluoroacetic acid (TFA) in HPLC-grade water. Solvent B was 0.1% (v/v) TFA in acetonitrile. The flow rate was regulated at 1 ml/min. Gradient conditions were as followed: 0.0% B for 2 mins, and then the percentage of B was increased to 60% over 30 min. Eluents were monitored at 215 nm. A typical load was 0.1 mg/ml of protein in water. All peaks obtained via rHPLC were collected, lyophilized to remove acetonitrile, and resolubilized in SDW or phosphate-buffered saline (PBS) for further analyses.

Mammalian cell bioassays

Immortalized human vaginal epithelial cells (HVECs; ATCC CRL-2616) were maintained as described previously (21). For all HVEC experiments, confluent monolayers of HVECs in 96-well plates were switched to antibiotic-free keratinocyte serum-free media the day before experimentation. Protein fractions (2 μg/fraction in 100 μl KSFM, unless otherwise noted) were added to the cell culture medium and incubated with HVECs at 37°C in the presence of 7% CO_2 for 19–24 h. At the end the experiments, the media were collected and stored at −20 °C until cytokine measurement. Interleukin-8 (IL-8) concentrations in the media were analyzed by enzyme-linked immunosorbent assay (ELISA). This cytokine was used as a measure of pro-inflammatory activity since IL-8 is a chemo-attractant for polymorphonuclear leukocytes (PMNs), the dominant mediators of acute inflammation. Cell viability was estimated by CellTiter 96 aqueous one solution cell proliferation assay (Promega, Madison, WI) according to manufacturer's instructions. All experiments were performed in duplicate to reserve enough proteins for downstream bioassays.

Protein analysis via mass spectrometry

Proteins (about 3 μg) obtained from the rHPLC samples were digested by trypsin, and peptide fragments were detected by tandem mass spectrum (MS/MS). Briefly, protein samples dissolved in water were subjected to in-solution trypsin digestion by trypsin 12 ng/μl in 25 mM ammonium bicarbonate/5 mM calcium chloride at 37 °C for 10 h. The digestion was terminated with the addition of formic acid to a final 0.1% v/v. Digested peptides were injected in a Michrom BioResources Paradigm 2D capillary LC system (Michrom Bioresources, Inc., Auburn, CA) online with LTQ ion trap mass spectrometer (ThermoFinnigan, San Jose, CA), a linear ion trap. Briefly, samples were loaded on a Paradigm Platinum Peptide Nanotrap precolumn (0.15 × 50 mm, 400 μl volume) and subsequently switched in-line with microcapillary columns (75 μm internal diameter, 12 cm in length) at a flow rate of approximately 350 nl/min. The capillary column was packed in-house with Magic C18 AQ reversed-phase material (5 μm, 200 Å pore size C18 particles). Peptides were eluted with a linear gradient with 100% solvent A (95:5 water: ACN, 0.1% formic acid), to a final solvent B (5:95 water: ACN, 0.1% formic acid). An electrospray voltage of 2250 V was applied distal to the analytic column. The LTQ was operated in the positive-ion mode using data-dependent acquisition methods initiated by a survey MS scan

NIH-PA Author Manuscript

NIH-PA Author Manuscript

NIH-PA Author Manuscript

which was followed by MS/MS (collision energy of 35%) on the 4 most abundant ions detected in the survey scan. M/Z values selected in the survey scan for MS/MS were excluded for subsequential MS/MS with a dynamic exclusion from further data-dependent MS/MS for 30 sec. The signal intensity threshold for an ion to be selected for MS/MS was set to a lower limit of 1000.

All MS/MS samples were analyzed using Sequest (ThermoFinnigan; version 27, rev. 13) and X! Tandem (www.thegpm.org; version 2007.01.01.1) searching the staphylococcus_NCBI_952306_CTM database assuming trypsin digestion. Sequest and X! Tandem were searched with a fragment ion mass tolerance of 1.00 Da and a parent ion tolerance of 0.80 Da. The Sequest search parameters were: carbamidomethyl modification of cysteine and differential for oxidation of methionine with 2 trypsin miscleavaged sites allowed. Scaffold (version Scaffold-02_02_03, Proteome Software Inc, Portland, OR) and ProteinPilot software version 3.0 was used to validate MS/MS-based peptide and protein identifications. Protein identifications were accepted if they had unused ProtScore equal or greater than 4 and at least 2 identified peptides with at least 99% probability.

Generation of rabbit anti-α-toxin sera

Dutch belted rabbits were immunized with 10 μg of the highly-purified α-toxin (from MNPE rHPLC peak 6) with Freund's incomplete adjuvant at times 0, day 14, and day 28. All animal experiments were performed in accordance with the University of Minnesota Institutional Animal Care and Use Committee (IACUC) protocol 0908A71722. Rabbit blood was obtained on day 35, and the anti-α-toxin was separated from blood and filter-sterilized with 0.2 μm filters. The anti-α-toxin antisera was used in hemolysin bioassay experiments for neutralization and Western immunoblotting.

Hemolysin bioassays

Hemolytic activity was evaluated on slides containing human or rabbit erythrocytes as described previously (22). Briefly, rabbit or human erythrocytes were washed three times with PBS. Microscope slides were coated with 4 ml of 0.8% agarose in PBS mixed with 0.6% erythrocytes (final concentration). Bacteria were grown overnight in beef heart medium supplemented with 1% glucose-phosphate buffer. Culture supernates were sterile filtered, added (20 μl) to the wells (4 mm diameter) and incubated at 37 °C for 6 h. Zones of lysis (clear zones) represent the amount of hemolysins in the sample. Zones of lysis were measured with a caliper to generate percent reduction.

Alpha-toxin Western immunoblotting

S. aureus secreted proteins purified by isoelectric focusing and rHPLC (CDC 587 peak 1: 60 μg) or sterile filtered overnight culture supernatants (5 μl) were mixed 1:1 with sample loading buffer and electrophoresed on a 12% acrylamide gel under reducing conditions, transferred onto polyvinylidene fluoride (PVDF) membranes, and immunoblotted with anti-α-toxin 7B8 monoclonal antibody (rHPLC, CDC 587 peak 1: 60 μg) (23) or antisera from rabbit (rabbit polyclonal antibodies against highly purified α-toxin isolated from MNPE, which were made by hyperimmunization of rabbits) (culture supernatants). Proteins were detected by chemiluminescence using SuperSignal West Dura Extended Duration substrate (Pierce), limit of detection (<0.075 μg/well).

Construction of *hla* mutants

The *hla::erm* mutation was transduced from strain DU1090 (24) into strains MN8, CDC587 and MNPE. Bacteriophage transductions were performed using F11 as described previously (25) and selection of the *hla::erm* mutation was performed on TSA with Erm. The presence

NIH-PA Author Manuscript

NIH-PA Author Manuscript

NIH-PA Author Manuscript

of *hla::erm* was confirmed by a 1.4 kb increase in size of the PCR product using primers hlaFwd (5′-atgaaaacacgtatagtcagc-3′) and hlaRev (5′-ttaatttgtcatttcttcttttttccc-3′) for the *hla* gene.

Rabbit model for α-toxin lethality

Ethics statement: All animal experiments were performed in accordance with the University of Minnesota IACUC protocol 0908A71722. Studies were performed in rabbits to determine the *in vivo* biological function of wild-type α-toxin (MNPE) versus mutant α-toxin (CDC587), where approximately 1 μg of α-toxin administered intravenously induces death in a rabbit within 15 min. This is a well-characterized activity of α-toxin (8), the only known staphylococcal protein with such activity. Rabbits (3/group; 12 total rabbits) were injected intravenously with 1 μg purified α-toxin, 2 ml of 0.2 μm filter-sterilized supernate from MNPE, 2 ml of 1× concentrated supernate from CDC587, or 2 ml of 10× concentrated supernate from CDC587. The CDC587 supernate was concentrated 10× by air-drying to 1/10 the original volume, followed by dialysis 24 h against PBS to remove excess salts. Animals were monitored up to 1 h for lethality. At the end of the experiment, animals were euthanized by barbiturate overdose (intravenous injection).

Calculations

Pro-inflammatory activity of an individual fraction was calculated by dividing IL-8 induction by the amount of the protein used in the assay (IL-8 induction/μg of protein). The total of pro-inflammatory activity in the fraction (IL-8/μg of protein × total protein in the fraction) is compared to the sum of the total pro-inflammatory activity from all the fractions (in the same IEF experiment). Due to all experiments only being performed in duplicate, data are presented as mean and the range of the duplicates.

RESULTS

Effects of *S. aureus* (MNPE and CDC587) on *ex vivo* porcine vaginal mucosa

Nearly all *S. aureus* induce diseases on mucosal and skin surfaces, unless the bacteria are implanted traumatically into the bloodstream. Previous studies to identify factors that facilitate *S. aureus* disease causation have focused typically on specific virulence factors. In an effort to take a more global approach, we assessed all virulence factors (exoproteins) secreted in vitro by two common USA200 methicillin-sensitive *S. aureus* strains: MNPE (wild-type α-toxin) was a representative strain for non-mucosal TSST-1^+ isolates, and CDC587 (α-toxin mutant) was a typical vaginal mucosal TSST-1^+ isolate. We began with porcine vaginal mucosa inoculated with *S. aureus* MNPE and CDC587 for 24 h. The surface of the porcine vaginal mucosa, like its human counterpart, is lined with stratified squamous epithelium. The surface epithelium of untreated control tissue remained intact, whereas the infected tissue showed signs of disruption (Fig 1). The surface epithelium damage in the MNPE infected tissue was several layers deep, and the epithelium exhibited signs of breakdown, whereas the damage due to CDC587 was minor and remained localized to the outermost layers of the infected tissue. Our prior studies suggest that these virulence factors are likely to be secreted exoproteins, rather than cell-surface associated factors (proteins) (26). Therefore, this histological analysis suggests that MNPE produced more vaginal tissue-damaging virulence factors than CDC587.

Differences in *S. aureus* (MNPE and CDC587) exoprotein profiles and induction of IL-8 from human vaginal epithelial cells (HVECs)

To examine our hypothesis that exoproteins contributed to the differences of *S. aureus* MNPE and CDC587 damage to vaginal mucosal tissue, total exoproteins (ammonium

NIH-PA Author Manuscript

NIH-PA Author Manuscript

NIH-PA Author Manuscript

sulfate-precipitated) in overnight culture supernates from MNPE and CDC587 were compared for their pro-inflammatory and cytotoxic effects on HVECs. IL-8, as a measure of pro-inflammatory potential, was increased approximately 19-fold (753 pg/ml) and 7-fold (295 pg/ml), compared to media controls, for MNPE and CDC587 total exoprotein (20 μg/ml; 2 μg of total protein/well), respectively (Fig. 2A). The corresponding survival of the HVECs to MNPE and CDC587 exoproteins (20 μg/ml) was 29% and 74%, respectively (Fig. 2B). Therefore, MNPE exoproteins were both more pro-inflammatory and more cytotoxic to HVECs than CDC587 exoproteins.

Distributions of biological activities for *S. aureus* (MNPE and CDC587) exoproteins

To identify the major MNPE and CDC587 exoproteins that contributed to the increased production of IL-8 and cytotoxicity, ammonium sulfate-precipitated exoproteins from overnight culture supernates were separated by thin-layer IEF. The initial IEF (pH 3–10) separated MNPE and CDC587 exoproteins into 15 fractions, and fractions 12 to 15 were determined to have the majority of biological activity (Fig. 3). MNPE fractions 12 to 15, corresponding pH 6.3–9.4, (20 μg/ml, 2 μg total protein/well) increased IL-8 production from HVECs by 5–15 fold, which accounted for more than 90% of the total pro-inflammatory activity (Fig. 3A). Corresponding CDC587 fractions 12–15, pH 6.4–10.1 (20 μg/ml) were less pro-inflammatory to HVECs (1–2 fold increase of IL-8) than MNPE fractions. These fractions from CDC587 contained 73% of the total pro-inflammatory activity for CDC587 exoproteins (Fig. 3B).

Since the majority of biological activity localized to a neutral to basic pH, second thin-layer IEFs of (pH 7–9) were applied to further separate proteins within the 12–15 fractions. The distributions of pro-inflammatory and cytotoxic activities of the fractionated MNPE and CDC587 samples by the second IEF are depicted in Fig. 4A and 4B, respectively. At the concentration of 20 μg/ml (2 μg total protein), all MNPE fractions were highly cytotoxic (>50% cytotoxicity; data not shown). Therefore, the relative pro-inflammatory responses of the fractions were compared at 2 μg/ml (0.2 μg total protein). MNPE fractions 10–15 (from pH 7–9 IEF) contained most of the biological activity: fractions 10–13 (pH 7.8–8.4) were highly pro-inflammatory and contained 82% of total inflammatory activity, while fractions 14–15 (pH 8.5–9.2) were cytotoxic and less inflammatory (contained 0.7% of the total pro-inflammatory activity) (Fig. 4A). At 20 μg/ml (2 μg total protein), CDC587 fractions from the pH 7–9 IEF were not highly inflammatory, inducing approximately 2-fold increases in IL-8 production. Fractions 11–15 (pH 7.6–9.0) from CDC587 were highly cytotoxic (18–51% cell viability), but not highly pro-inflammatory to HVECs (Fig. 4B). These fractions accounted for 87% of the total pro-inflammatory activity of all pH 7–9 IEF CDC587 fractions. The CDC587 fractions were neither pro-inflammatory nor cytotoxic (>50% cell survival) at the concentration of 2 μg/ml (data not shown).

In general, MNPE fractions from the pH 7–9 IEF were more hemolytic (another measure of cytotoxic activity) to rabbit erythrocytes than human erythrocytes (Fig. 4C). In contrast, CDC587 fractions pH 7–9 IEF (at the same total protein concentration) were hemolytic to both rabbit and human erythrocytes at similar levels, although overall they were not as hemolytic as MNPE pH 7–9 IEF fractions (Fig. 4D).

Fractions from the pH 7–9 IEF were grouped and further resolved by rHPLC based on their protein patterns appearing on silver-stained SDS-PAGE gels (data not shown). The grouping was to maximize the amount of proteins recovered from rHPLC. Only rHPLC peaks with more than 10 μg total proteins were tested for biological activity and evaluated for protein identification by mass spectrometry. There were 6 peaks from MNPE pH 7–9 IEF fractions that were tested: peaks 1 to 3 from fractions 4–7 (pH 6.8–7.5), peaks 4 and 5 from fractions 10–12 (pH 7.8–8.2), and peak 6 from fractions 13–15 (pH 8.4–9.2) (Fig. 5). There were 5

NIH-PA Author Manuscript

NIH-PA Author Manuscript

NIH-PA Author Manuscript

peaks from CDC587 pH 7–9 IEF fractions that were tested: peaks 1 and 2 from fractions 7–10 (pH 6.1–7.2), and peaks 3 to 5 from fractions 13–15 (pH 8.1–9.0) (Fig. 6). One peak from CDC587 pH 7–9 fractions 7–10 was determined to contain 20 μg total protein by Bradford protein assay but could not be detected by silver-stained SDS-PAGE. Therefore, the peak was also excluded from further assays. None of the peaks recovered from CDC587 fractions 11–12 (pH 7.6–8.0) were pro-inflammatory to HVECs at the concentration of 20 μg/ml. Therefore, these peaks were not shown.

MNPE peaks 2, 5, and 6 were highly pro-inflammatory to HVECs at concentrations higher than 2 μg/ml, while peak 3 was highly pro-inflammatory at a concentration of 20 μg/ml (Fig. 5B). Peak 3 had weak bands within the mass range of 25 to 75 kDa but a strong band at the gel front (not shown). Therefore, the pro-inflammatory activity may be contributed by non-protein contents, small proteins, or protein fragments. At the concentration of 20 μg/ml, peaks 3, 5, and 6 were relatively more cytotoxic to HVECs than other peaks, although all of them had > 50% cell survival (Fig. 5C). In contrast, CDC587 peaks contained more varieties of proteins than MNPE peaks (Fig. 6A). Peaks 3 and 4 were highly pro-inflammatory at the concentration ≥ 2 μg/ml, whereas peak 5 was only highly pro-inflammatory at the concentration of 20 μg/ml (Fig. 6B). These peaks tended to be more cytotoxic than other peaks in the group, but all of them had >50% cell survival (Fig. 6C).

Identification of USA200 *S. aureus* exoproteins associated with virulence via mass spectrometry

All rHPLC peaks examined above were treated with in-solution digestion and identified via mass spectrometry analyses individually. Multiple proteins were detected in each sample, and several proteins were detected in multiple samples. Tables 1 and 2 list the total virulence-associated proteins (exoenzymes and exotoxins) detected from the MNPE and CDC587 peaks, respectively.

Fewer total proteins were identified from MNPE peaks than CDC587 peaks. There were 9 virulence-associated proteins detected from MNPE peaks, including those hypothesized to be involved in staphylococcal pathogenesis, such as lipase, nuclease, staphylococcal complement inhibitor, staphylokinase, staphopain A, trypsin-like serine protease (probably V8), α-toxin, TSST-1, SEC, and possibly other enterotoxin(s) (Table 1). The density of the bands at specific molecular weights on SDS-PAGE gel suggested that TSST-1, SEC, and α-toxin were made in higher concentrations than other exoproteins (Fig. 5A). In contrast, there were 24 virulence-associated proteins identified from CDC587 peaks (Table 2). In addition to those virulence-associated exoproteins identified in MNPE peaks, there were chemotaxis inhibitor protein CHIPS, MHC II-like molecule, and 1-phosphatidylinostitol phosphodiesterase, signal transduction protein TRAP, secretory antigen ssaA-like protein, and staphylococcal accessory regulator T. There were two subtypes of lipases, lip1 and lip 2, detected in the fractions. Cell wall-associated virulence proteins including iron-regulated hemo-iron binding protein, fibronectin-binding protein, and a surface protein with 5′-nucleotidase were also detected. Exotoxins including beta-type phenol soluble modulin, γ-toxin, TSST-1, SEC, and α-toxin were also identified from CDC587 (Table 2).

Alpha-toxin (highly purified in MNPE peak 6) was therefore identified as the single most pro-inflammatory and cytotoxic protein purified (Fig. 5). SEC (highly purified in MNPE peaks 1 and 4) was found to be less pro-inflammatory than TSST-1 (highly purified in CDC587 peak 1) to HVECs at the concentration up to 20 μg/ml (Fig. 6). Pro-inflammatory activity of CDC587 peaks 3 and 4 were likely induced by the mixtures of α-toxin and γ-toxin. Pro-inflammatory activity of CDC587 peak 5 was likely due to staphopain A (Fig. 6). CDC587 fractions 1, 3 to 5 were detected to contain α-toxin with 45%, 70%, 55%, 51%

NIH-PA Author Manuscript

NIH-PA Author Manuscript

NIH-PA Author Manuscript

sequence (total peptide) coverage, respectively. The identified peptides were located at both sides of the stop codon (CAG [Gln] to TAG [stop codon]) at codon 113.

Evidence of functionally active α-toxin

Previous data are conflicting on whether or not functional α-toxin can be produced by USA200 strains with a stop codon in the *hla* structural gene (*hla*¯). The mass spectrometry analyses of the CDC587 fractions indicated the presence of peptides that corresponded to the amino acid sequence of α-toxin, despite the presence of the stop codon in the chromosome. Similar exotoxin purification and protein identification studies (ie., IEF, HPLC and mass spectrometry) of an additional USA200 strain with mutant *hla* (*hla*¯) (*S. aureus* MN8) were conducted, and these studies confirmed that strain MN8 also produces α-toxin despite a stop codon in *hla*.

Although no α-toxin was visible in CDC587 peak 1 from rHPLC on the 12% SDS-PAGE in Fig. 6A, this peak had the highest protein concentration and was not detected to have other hemolysins (i.e. γ-toxin) by mass spectrometry. Therefore, this peak was chosen for Western immunoblotting. Nearly 250-fold more protein was loaded onto the gel and indeed, the Western blot probed with anti-α-toxin MAb demonstrates that CDC587 produced α-toxin (Fig. 7A).

Evidence of biologically active α-toxin is depicted in Fig. 7B. A rabbit erythrocyte hemolysis assay was performed using overnight culture supernates from wild-type and α–toxin knockouts (ko) of MNPE, CDC587 and MN8. As expected, wild-type MNPE was more hemolytic than CDC587 and MN8 wild type (wt) strains. Targeted deletion of the α–toxin gene resulted in reductions in the zone of hemolysis by each of the strains examined. The largest reduction was observed in the MNPEko strain compared to MNPEwt (29.9%) The reduction of hemolysis observed in the MN8ko strain was intermediate at 18.7%. Knocking out the α-toxin gene in CDC587 resulted in a 10.5% reduction in hemolysis.

Absence of α-toxin protein was confirmed in 2 of the 3 knock out strains by Western blot analysis (Fig. 7C). Proteins from overnight culture supernatants of MNPE, MN8 and their corresponding ko strains were separated by 12% SDS-PAGE and immunoblotted with a polyclonal rabbit anti-α-toxin. Bands corresponding to α-toxin are visible in the wild-type strains and absent in the lanes containing supernatants from the knock-out strains. The amount of α-toxin present in CDC587wt and CDC587ko overnight filtered culture supernatants was below the limit of detection (<0.075 μg/well). Detection of α-toxin in CDC587 strains was further complicated by excessive amounts of secreted protein A, which obscured the α-toxin band (data not shown).

In addition, rabbits (not immunized against alpha toxin) challenged with either un-concentrated MNPE supernatants or 10-fold concentrated CDC587 overnight culture supernatants intravenously died within 30 min of intravenous injection (3/3 per group), which was comparable to rabbits that received 1 μg of highly-purified α-toxin. In contrast, un-concentrated supernatants from CDC587 did not induce lethality.

DISCUSSION

S. aureus is a highly versatile microorganism, capable of colonizing human mucosal and skin surfaces, as well as producing exotoxins and other factors that cause local tissue damage and systemic diseases such as TSS. The organisms can also cause systemic diseases through traumatic implantation into the circulation (27). In an effort to estimate the overall contributions of all secreted *S. aureus* exoproteins, individually and in combination, to cause inflammation to mucosal barriers or damage epithelial tissue integrity directly, we

NIH-PA Author Manuscript

NIH-PA Author Manuscript

NIH-PA Author Manuscript

conducted a global characterization of pro-inflammatory and cytotoxic proteins from two MSSA USA200 TSS strains. These strains are representative of the most common methicillin-sensitive strains of *S. aureus* that colonize humans and are associated with TSS (4–5); the USA200 designation is based on pulsed-field gel electrophoresis profile as defined by the Centers for Disease Control and Prevention.

By serial separations, which were based on biochemical properties of the proteins and mass spectrometry, we have separated and identified major staphylococcal exoproteins responsible for pro-inflammatory responses and cytotoxicity to epithelial cells. CDC587 was found to produce more total virulence factors than MNPE; however, most of these virulence factors were produced at low levels. Cytolysins (α-toxin and γ-toxin), superantigens (i.e. TSST-1 and SEC), staphylokinase, and staphopain A were identified from both isolates. Alpha-toxin, γtoxin, TSST-1, and potentially staphopain A were identified as major staphylococcal exoproteins that contribute to pro-inflammatory and cytotoxicity activities from epithelial cells by the USA200 isolates, and α-toxin was the main exoprotein responsible for the greater cytotoxicity and pro-inflammatory activity to HVECs in MNPE culture supernates, compared to CDC587. This study also determined that despite both MNPE and CDC587 containing genes for numerous SAgs, including TSST-1, SEA, SEC and SEl-G, -K, -M, -O, -P; only two SAgs, TSST-1 and SEC, were produced in high enough concentrations to be purified and possess biological activity to epithelial cells. As previously reported, these two SAgs, TSST-1 and SEC, together with SEB are associated with most cases of TSS (28–31).

In the present study, MNPE, a strain isolated from a lethal pneumonia TSS case and likely originating from a skin source, was found to produce a large amount of α-toxin and superantigens but not many other secreted virulence factors, whereas CDC587, a stereotypical menstrual vaginal mucosal TSS isolate, produced a wide variety of secreted virulence factors. Our group has previously shown that menstrual vaginal mucosal TSS *S. aureus* isolates produce significantly less α-toxin than skin organisms (10–11). It is possible that a strain that produces less α-toxin, such as CDC587, is more suitable for mucosal colonization, whereas high-level α-toxin production by MNPE makes the organism more suitable for skin colonization. Therefore, we hypothesize that strains, which produce large amount of α-toxin such as MNPE, are selected for survival on intact skin, whereas strains producing a minimal amount of α-toxin, such as CDC587, are selected for nasal or other mucosal surface colonization. The basis for this difference was the difficulty to colonize skin, such that high levels of α-toxin are required to cause dermonecrosis with consequent production of a colonization site (furuncle). Thus, organisms such as MNPE produce a large amount of α-toxin and TSST-1, two toxins that appear essential to the organism. In contrast, high-level production of α-toxin on mucosal surfaces would be predicted to result in exceptionally high-fatality due to sepsis and/or high-level exotoxin penetration into the circulation; this may have accounted for MNPE causing a fatal case of post-influenza TSS. Also, the emerging skin strains of MRSA, including USA300 and USA400 organisms, have been accompanied by high-level production of cytolysins, presumably necessary for production of the large numbers of abscesses associated with the infections (7, 32). These same organisms are associated with highly fatal necrotizing pneumonia in humans, consistent with their lack of fitness to mucosal surfaces. Even though USA200 organisms such as CDC587 have the ability to cause mucosal TSS, far more individuals are colonized with the organism than develop TSS. This fact suggests that USA200 organisms are selected by their mucosal environment for the production of those virulence factors that favor colonization without causing serious disease.

Various mechanisms of genetic selection have been described for other organisms in various environments. For example, *Pseudomonas aeruginosa* developed genetic mutations, that

NIH-PA Author Manuscript

NIH-PA Author Manuscript

NIH-PA Author Manuscript

result in a mucoid phenotype, to maintain chronic lung infections in patients with cystic fibrosis (33). The combinations of plasminogen-binding M protein and plasminogen activator streptokinase genetic variants have been associated with the fitness of *Streptococcus pyogenes* isolates on the skin or throat (34). Josefsson and colleagues have shown that *S. aureus* transcription levels of virulence factors are also affected by the surrounding tissues in a mouse septic arthritis model (35). Therefore, *S. aureus* isolates may be affected by their environmental niches (skin or mucosal surfaces) through selection of certain virulence proteins that are down-regulated due to the detrimental effects of excessive immune responses. An example of this may be the presence of the stop codon in the α-toxin gene. Thus, CDC587 and related isolate (MN8) utilize a read-through mechanism to enable low-levels of α-toxin production. The paucity of production of secreted virulence factors by strain MNPE, compared to production of large numbers by CDC587 may be another example of *S. aureus* niche-specific selection.

In addition to α-toxin and superantigens, γ-toxin and the protease staphopain A were also indicated to be pro-inflammatory molecules to epithelial cells in our study. Gamma-toxin, α-toxin, and Panton Valentine leukocidin (PVL), a cytolysin epidemiologically associated with severe skin infections in the community, all belong to the heptamer pore-forming cytolysin family. Gamma-toxin and PVL are hetero-chain heptamers, whereas α-toxin is a homo-chain heptamer; these structural differences may account for their observed activity differences (36). Similar to α-toxin, γ-toxin has been suggested to play a role in a rabbit *S. aureus* keratitis model (37). Our data indicate that menstrual TSS isolates such as CDC587 and related isolates produce relatively more γ-toxin than MNPE. The role of γ-toxin in *S. aureus* TSS pathogenesis has not been well characterized.

Staphopain A is a cysteine protease that has been shown to induce vascular leakage in guinea pig skin, which potentially facilitates septic shock (38). Our data indicate that this protease is pro-inflammatory to epithelial cells and thereby important for *S. aureus* pathogenesis on mucosal surfaces. Other secreted virulence factors were identified in our studies, including staphylococcal inhibitor of complement, which inhibits complement; staphylokinase, which inhibits host antimicrobial peptide α-defensins (39); lipases, and nucleases. These secreted proteins were not shown to be pro-inflammatory to epithelial cells in our study.

Rabbit red blood cells are highly sensitive to both α- and γ-toxin, while human red blood cells are more sensitive to γ-toxin than α-toxin (> 50-fold different) (40). These differences observed in hemolytic profiles are consistent with our results, which indicated MNPE and CDC587 produced different amounts and types of hemolysins (MNPE α-toxin vs. CDC587 possibly α- and γ-toxins) and warranted further study.

Interestingly, despite the nonsense mutation in α-toxin, CDC587 and related organism (MN8) still produced small amounts of α-toxin, indicating translational read-through in these *S. aureus* strains. Our studies have provided several pieces of evidence that these strains produce functional α-toxin, albeit at a low-level: 1) mass spectrometry; 2) α-toxin Western blot; 3) reduction of red cell lysis in α-toxin KO strains; and 4) *in vivo* toxicity in rabbits. Stop codon read-through mechanism(s) in *S. aureus* have not been characterized previously. Nonetheless, read-through of an amber stop codon (UAG) has been fully characterized in many organisms, including *Escherichia coli*, *Saccharomyces cerevisiae*, where the read-through is sufficient for the organism to produce enough essential proteins such that normal growth occurs (41–42).

Our group has previously reported the synergic effects of α-toxin and TSST-1 to promote pro-inflammatory responses and cytotoxicity from epithelial cells, which allows mucosal

NIH-PA Author Manuscript

NIH-PA Author Manuscript

NIH-PA Author Manuscript

penetration of TSST-1 to cause TSS (9). Alpha-toxin was also determined to contribute to the majority of tissue damage in a murine pneumonia model, which is not sensitive to superantigens (7). Our studies therefore support the previous findings that α-toxin plays important roles in *S. aureus* illnesses and suggest that α–toxin may play a more widespread role in the burden of staphylococcal disease than previously thought.

This study was a global characterization of exoproteins important for inducing cytokines from epithelial cells and causing epithelial cell death. We identified several exoproteins that may play important roles in establishing *S. aureus* disease on mucosal surfaces. The differences in the secreted virulence factor profiles between these two genetically related strains also suggest that production of virulence factors can vary considerably based on the host environmental niche from which the strains were isolated. Identification of the important role of these exoproteins as performed in this study is an important step towards development of vaccines, prophylactics, and enhanced therapeutics designed to control *S. aureus* diseases, including TSS. Further we demonstrated production of biologically active α–toxin in spite of the presence of a nonsense mutation in the gene.

Acknowledgments

We gratefully acknowledge the mass spectrometry core laboratory in the University of Minnesota for their assistance in protein identification and analyses. We also thank Juliane Bubeck Wardenburg (Departments of Pediatrics and Microbiology, University of Chicago, Chicago, IL 60637) for contributing anti-α-toxin 7B8 monoclonal antibody used in Western blot analyses.

ABBREVIATIONS AND TEXTUAL FOOTNOTES

CFU	Colony-forming units
ELISA	Enzyme-linked immunosorbent assay
erm	Erythromycin resistance gene
HVECs	Human vaginal epithelial cells
IACUC	Institutional Animal Care and Use Committee
IL-8	Interleukin 8
IEF	Isoelectric focusing
IU	International unit
KSFM	Keratinocyte serum-free media
KO	Knockout
MHC	Major histocompatibility complex
MS	Mass spectrum
MSSA	Methicillin-sensitive *S. aureus*
MRSA	Methicillin-resistant *S. aureus*
MW	Molecular weight
MAb	Monoclonal antibody
PVL	Panton-Valentine leukocidin
PMNs	Polymorphonuclear leukocytes
PVDF	Polyvinylidene fluoride

NIH-PA Author Manuscript

NIH-PA Author Manuscript

NIH-PA Author Manuscript

PCR	Polymerase chain reaction
PFGE	Pulsed-field gel electrophoresis
RBCs	Red blood cells
rHPLC	Reverse phase high performance liquid chromatography
SDW	Sterile distilled water
SDS-PAGE	Sodium dodecyl sulfate polyacrylamide gel electrophoresis
SE	Staphylococcal enterotoxin
SEl	Staphylococcal enterotoxin-like
MS/MS	Tandem mass spectrum
TSS	Toxic shock syndrome
TSST-1	Toxic shock syndrome toxin 1
TFA	Trifluoroacetic acid
WT	Wild-type

References

1. Kuehnert MJ, Hill HA, Kupronis BA, Tokars JI, Solomon SL, Jernigan DB. Methicillin-resistant-*Staphylococcus aureus* hospitalizations, United States. Emerg Infect Dis. 2005; 11:868–872. [PubMed: 15963281]
2. Gorwitz RJ, Kruszon-Moran D, McAllister SK, McQuillan G, McDougal LK, Fosheim GE, Jensen BJ, Killgore G, Tenover FC, Kuehnert MJ. Changes in the prevalence of nasal colonization with *Staphylococcus aureus* in the United States, 2001–2004. J Infect Dis. 2008; 197:1226–1234. [PubMed: 18422434]
3. Wertheim HF, Melles DC, Vos MC, van Leeuwen W, van Belkum A, Verbrugh HA, Nouwen JL. The role of nasal carriage in *Staphylococcus aureus* infections. Lancet Infect Dis. 2005; 5:751–762. [PubMed: 16310147]
4. Tenover FC, McAllister S, Fosheim G, McDougal LK, Carey RB, Limbago B, Lonsway D, Patel JB, Kuehnert MJ, Gorwitz R. Characterization of *Staphylococcus aureus* isolates from nasal cultures collected from individuals in the United States in 2001 to 2004. J Clin Microbiol. 2008; 46:2837–2841. [PubMed: 18632911]
5. Wertheim HF, van Leeuwen WB, Snijders S, Vos MC, Voss A, Vandenbroucke-Grauls CM, Kluytmans JA, Verbrugh HA, van Belkum A. Associations between *Staphylococcus aureus* Genotype, Infection, and InHospital Mortality: A Nested Case-Control Study. J Infect Dis. 2005; 192:1196–1200. [PubMed: 16136462]
6. Peacock SJ, Moore CE, Justice A, Kantzanou M, Story L, Mackie K, O'Neill G, Day NP. Virulent combinations of adhesin and toxin genes in natural populations of *Staphylococcus aureus*. Infect Immun. 2002; 70:4987–4996. [PubMed: 12183545]
7. Bubeck Wardenburg J, Schneewind O. Vaccine protection against *Staphylococcus aureus* pneumonia. J Exp Med. 2008; 205:287–294. [PubMed: 18268041]
8. Bhakdi S, Tranum-Jensen J. Alpha-toxin of *Staphylococcus aureus*. Microbiol Rev. 1991; 55:733–751. [PubMed: 1779933]
9. Brosnahan AJ, Mantz MJ, Squier CA, Peterson ML, Schlievert PM. Cytolysins augment superantigen penetration of stratified mucosa. J Immunol. 2009; 182:2364–2373. [PubMed: 19201891]
10. O'Reilly M, Kreiswirth B, Foster TJ. Cryptic alpha-toxin gene in toxic shock syndrome and septicaemia strains of *Staphylococcus aureus*. Mol Microbiol. 1990; 4:1947–1955. [PubMed: 2082151]

NIH-PA Author Manuscript

NIH-PA Author Manuscript

NIH-PA Author Manuscript

11. Schlievert PM, Osterholm MT, Kelly JA, Nishimura RD. Toxin and enzyme characterization of *Staphylococcus aureus* isolates from patients with and without toxic shock syndrome. Ann Intern Med. 1982; 96:937–940. [PubMed: 7091971]
12. Hecker M, Engelmann S, Cordwell SJ. Proteomics of *Staphylococcus aureus*--current state and future challenges. J Chromatogr B Analyt Technol Biomed Life Sci. 2003; 787:179–195.
13. Burlak C, Hammer CH, Robinson MA, Whitney AR, McGavin MJ, Kreiswirth BN, Deleo FR. Global analysis of community-associated methicillin-resistant *Staphylococcus aureus* exoproteins reveals molecules produced in vitro and during infection. Cell Microbiol. 2007; 9:1172–1190. [PubMed: 17217429]
14. MacDonald KL, Osterholm MT, Hedberg CW, Schrock CG, Peterson GF, Jentzen JM, Leonard SA, Schlievert PM. Toxic shock syndrome. A newly recognized complication of influenza and influenzalike illness. Jama. 1987; 257:1053–1058. [PubMed: 3806893]
15. Schlievert PM, Shands KN, Dan BB, Schmid GP, Nishimura RD. Identification and characterization of an exotoxin from *Staphylococcus aureus* associated with toxic-shock syndrome. J Infect Dis. 1981; 143:509–516. [PubMed: 6972418]
16. Schlievert PM, Case LC, Strandberg KL, Tripp TJ, Lin YC, Peterson ML. Vaginal *Staphylococcus aureus* superantigen profile shift from 1980 and 1981 to 2003, 2004, and 2005. J Clin Microbiol. 2007; 45:2704–2707. [PubMed: 17537948]
17. Squier CA, Mantz MJ, Schlievert PM, Davis CC. Porcine vagina ex vivo as a model for studying permeability and pathogenesis in mucosa. J Pharm Sci. 2008; 97:9–21. [PubMed: 17721937]
18. Anderson MJ, Horn ME, Lin YC, Parks PJ, Peterson ML. Efficacy of concurrent application of chlorhexidine gluconate and povidone iodine against six nosocomial pathogens. Am J Infect Control. 38:826–831. [PubMed: 21035920]
19. Yarwood JM, Schlievert PM. Oxygen and carbon dioxide regulation of toxic shock syndrome toxin 1 production by *Staphylococcus aureus* MN8. J Clin Microbiol. 2000; 38:1797–1803. [PubMed: 10790102]
20. Bradford MM. A rapid and sensitive method for the quantitation of microgram quantities of protein utilizing the principle of protein-dye binding. Anal Biochem. 1976; 72:248–254. [PubMed: 942051]
21. Fichorova RN, Rheinwald JG, Anderson DJ. Generation of papillomavirus-immortalized cell lines from normal human ectocervical, endocervical, and vaginal epithelium that maintain expression of tissue-specific differentiation proteins. Biol Reprod. 1997; 57:847–855. [PubMed: 9314589]
22. Peterson ML, Schlievert PM. Glycerol monolaurate inhibits the effects of Gram-positive select agents on eukaryotic cells. Biochemistry. 2006; 45:2387–2397. [PubMed: 16475828]
23. Ragle BE, Bubeck Wardenburg J. Anti-alpha-hemolysin monoclonal antibodies mediate protection against *Staphylococcus aureus* pneumonia. Infect Immun. 2009; 77:2712–2718. [PubMed: 19380475]
24. O'Reilly M, de Azavedo JC, Kennedy S, Foster TJ. Inactivation of the alpha-haemolysin gene of *Staphylococcus aureus* 8325-4 by site-directed mutagenesis and studies on the expression of its haemolysins. Microb Pathog. 1986; 1:125–138. [PubMed: 3508485]
25. Novick RP. Genetic systems in staphylococci. Methods Enzymol. 1991; 204:587–636. [PubMed: 1658572]
26. Peterson ML, Ault K, Kremer MJ, Klingelhutz AJ, Davis CC, Squier CA, Schlievert PM. The innate immune system is activated by stimulation of vaginal epithelial cells with *Staphylococcus aureus* and toxic shock syndrome toxin 1. Infect Immun. 2005; 73:2164–2174. [PubMed: 15784559]
27. Lowy FD. Staphylococcus aureus infections. N Engl J Med. 1998; 339:520–532. [PubMed: 9709046]
28. Schlievert PM. Staphylococcal enterotoxin B and toxic-shock syndrome toxin-1 are significantly associated with non-menstrual TSS. Lancet. 1986; 1:1149–1150. [PubMed: 2871397]
29. Crass BA, Bergdoll MS. Involvement of staphylococcal enterotoxins in nonmenstrual toxic shock syndrome. J Clin Microbiol. 1986; 23:1138–1139. [PubMed: 3711305]
30. Crass BA, Bergdoll MS. Toxin involvement in toxic shock syndrome. J Infect Dis. 1986; 153:918–926. [PubMed: 3701106]

NIH-PA Author Manuscript

NIH-PA Author Manuscript

NIH-PA Author Manuscript

31. Bohach GA, Kreiswirth BN, Novick RP, Schlievert PM. Analysis of toxic shock syndrome isolates producing staphylococcal enterotoxins B and C1 with use of southern hybridization and immunologic assays. Rev Infect Dis. 1989; 11(Suppl 1):S75–81. discussion S81–72. [PubMed: 2494691]
32. Montgomery CP, Boyle-Vavra S, Adem PV, Lee JC, Husain AN, Clasen J, Daum RS. Comparison of virulence in community-associated methicillin-resistant *Staphylococcus aureus* pulsotypes USA300 and USA400 in a rat model of pneumonia. J Infect Dis. 2008; 198:561–570. [PubMed: 18598194]
33. Smith EE, Buckley DG, Wu Z, Saenphimmachak C, Hoffman LR, D'Argenio DA, Miller SI, Ramsey BW, Speert DP, Moskowitz SM, Burns JL, Kaul R, Olson MV. Genetic adaptation by *Pseudomonas aeruginosa* to the airways of cystic fibrosis patients. Proc Natl Acad Sci U S A. 2006; 103:8487–8492. [PubMed: 16687478]
34. Kalia A, Bessen DE. Natural selection and evolution of streptococcal virulence genes involved in tissue-specific adaptations. J Bacteriol. 2004; 186:110–121. [PubMed: 14679231]
35. Josefsson E, Kubica M, Mydel P, Potempa J, Tarkowski A. In vivo sortase A and clumping factor A mRNA expression during *Staphylococcus aureus* infection. Microb Pathog. 2008; 44:103–110. [PubMed: 17890045]
36. Diep BA, Otto M. The role of virulence determinants in community-associated MRSA pathogenesis. Trends Microbiol. 2008; 16:361–369. [PubMed: 18585915]
37. Dajcs JJ, Thibodeaux BA, Girgis DO, O'Callaghan RJ. Corneal virulence of *Staphylococcus aureus* in an experimental model of keratitis. DNA Cell Biol. 2002; 21:375–382. [PubMed: 12167239]
38. Imamura T, Tanase S, Szmyd G, Kozik A, Travis J, Potempa J. Induction of vascular leakage through release of bradykinin and a novel kinin by cysteine proteinases from *Staphylococcus aureus*. J Exp Med. 2005; 201:1669–1676. [PubMed: 15897280]
39. Jin T, Bokarewa M, Foster T, Mitchell J, Higgins J, Tarkowski A. Staphylococcus aureus resists human defensins by production of staphylokinase, a novel bacterial evasion mechanism. J Immunol. 2004; 172:1169–1176. [PubMed: 14707093]
40. Mollby R, Wadstrom T. Separation of Gamma Hemolysin from *Staphylococcus aureus* Smith 5R. Infect Immun. 1971; 3:633–635. [PubMed: 16558028]
41. Belin D. Why are suppressors of amber mutations so frequent among *Escherichia coli* K12 strains?. A plausible explanation for a long-lasting puzzle. Genetics. 2003; 165:455–456. [PubMed: 14573460]
42. von der Haar T, Tuite MF. Regulated translational bypass of stop codons in yeast. Trends Microbiol. 2007; 15:78–86. [PubMed: 17187982]

NIH-PA Author Manuscript

NIH-PA Author Manuscript

NIH-PA Author Manuscript

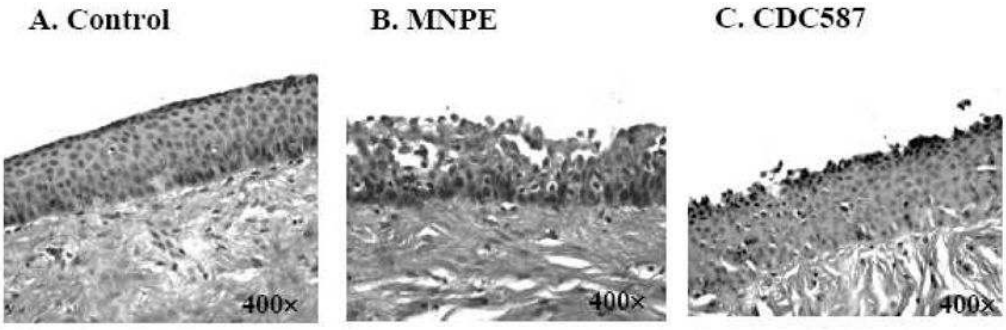

Figure 1. Effects of *S. aureus* on *ex vivo* porcine vaginal epithelium

The tissue was inoculated with 10^7 CFU *S. aureus* for 24 h and stained with hematoxylin and eosin. (A) Control, (B) *S. aureus* MNPE, (C) *S. aureus* CDC587.

NIH-PA Author Manuscript

NIH-PA Author Manuscript

NIH-PA Author Manuscript

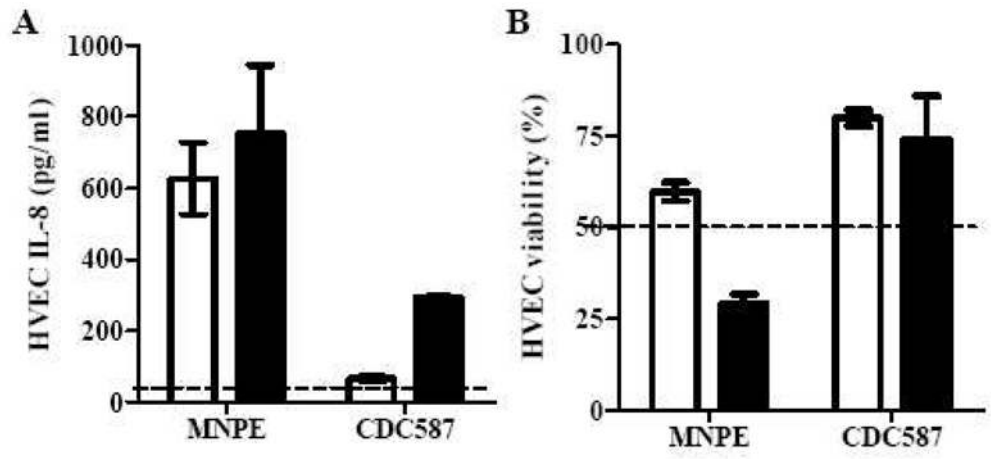

Figure 2. Effects of *S. aureus* exoproteins on human vaginal epithelial cells (HVECs)

HVEC IL-8 production (A) and viability (B) caused by different concentrations of *S. aureus* MNPE and CDC587 exoproteins. Open bars represent 2 μg/ml; closed bars represent 20 μg/ml; Dashed line represents the IL-8 level in the media control (A), and 50% viability (ie., LD_{50}) (B); The data were presented as mean ± range of the duplicates.

NIH-PA Author Manuscript

NIH-PA Author Manuscript

NIH-PA Author Manuscript

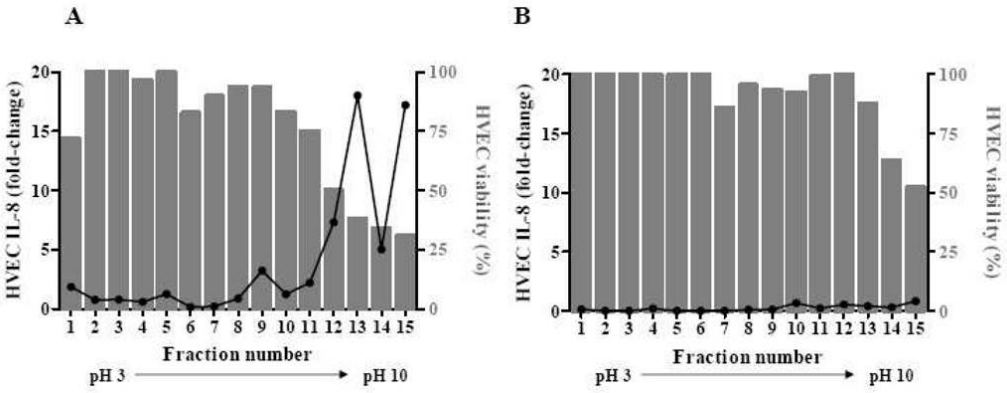

Figure 3. Distribution of biological activities in *S. aureus* pH 3–10 IEF fractions 1 to 15

HVECs were incubated with 20 μg/ml of fractionated exoproteins from MNPE (A) or CDC587 (B). Bars represent HVEC viability, and the line represents relative IL-8 secreted in the supernates compared to media control (fold-change).

NIH-PA Author Manuscript

NIH-PA Author Manuscript

NIH-PA Author Manuscript

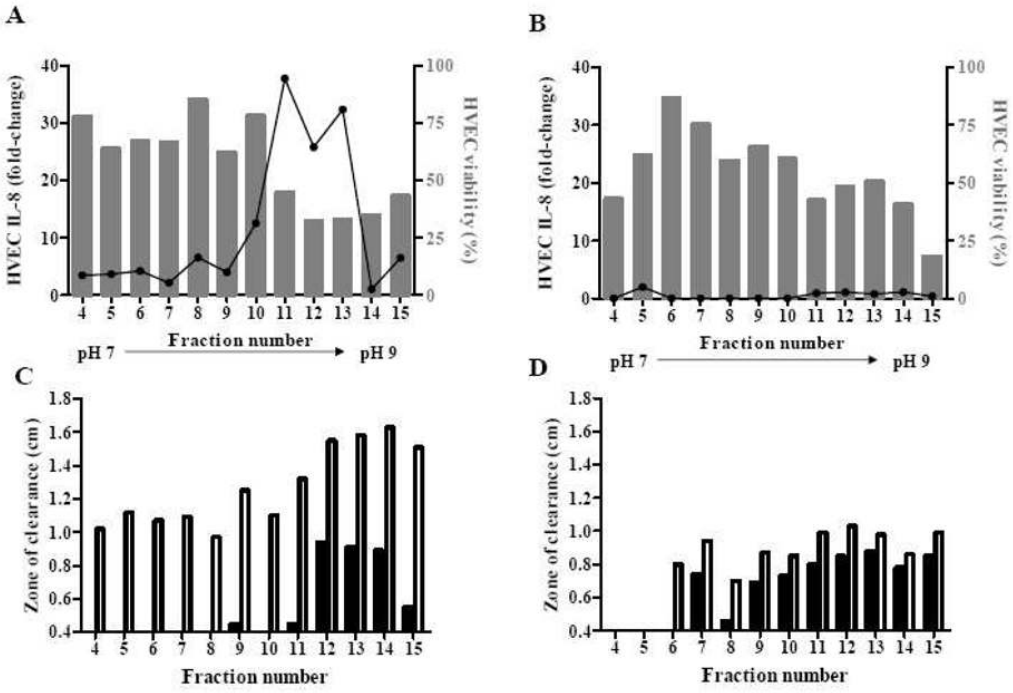

Figure 4. Distribution of biological activities from *S. aureus* pH 7–9 IEF fractions 4–15

HVECs were incubated with 2 μg/ml of MNPE proteins (A) or 20 μg/ml of CDC587 proteins (B) fractionated from IEF pH 7–9. Bars represent HVEC viability, and the line represents relative IL-8 secreted in the supernates compared to growth control. Hemolytic ability of 2.5 μg fractionated MNPE (C) and CDC587 (D) to human (closed bar) and rabbit (open bar) red blood cells.

NIH-PA Author Manuscript

NIH-PA Author Manuscript

NIH-PA Author Manuscript

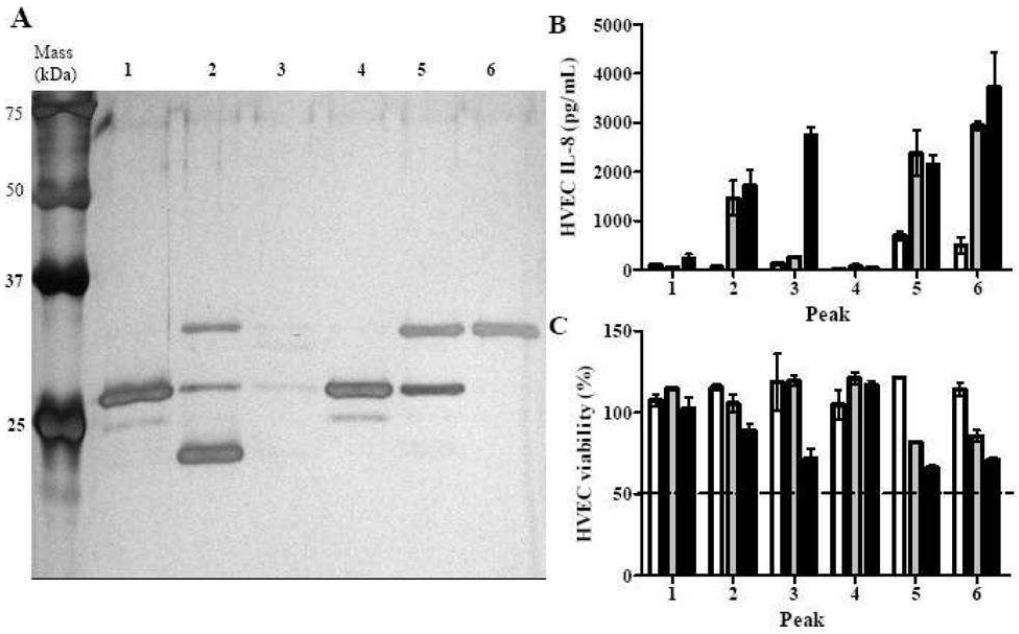

Figure 5. Proteins and biological activities in peaks of MNPE pH 7–9 IEF fractions after rHPLC separation

(A) Peaks from rHPLC (approximately 250 ng) separated by 12% SDS-PAGE. Proteins on the gel were identified according to molecular mass and mass spectrometry of the rHPLC peaks (Tables 1 and 2). (B) IL-8 production by HVECs treated with MNPE rHPLC peaks. (C) Viability of HVECs treated with MNPE rHPLC peaks. (open bar, 0.2 μg/ml; gray bar, 2 μg/ml; closed bar, 20 μg/ml). The data were presented as mean ± range of the duplicates.

NIH-PA Author Manuscript

NIH-PA Author Manuscript

NIH-PA Author Manuscript

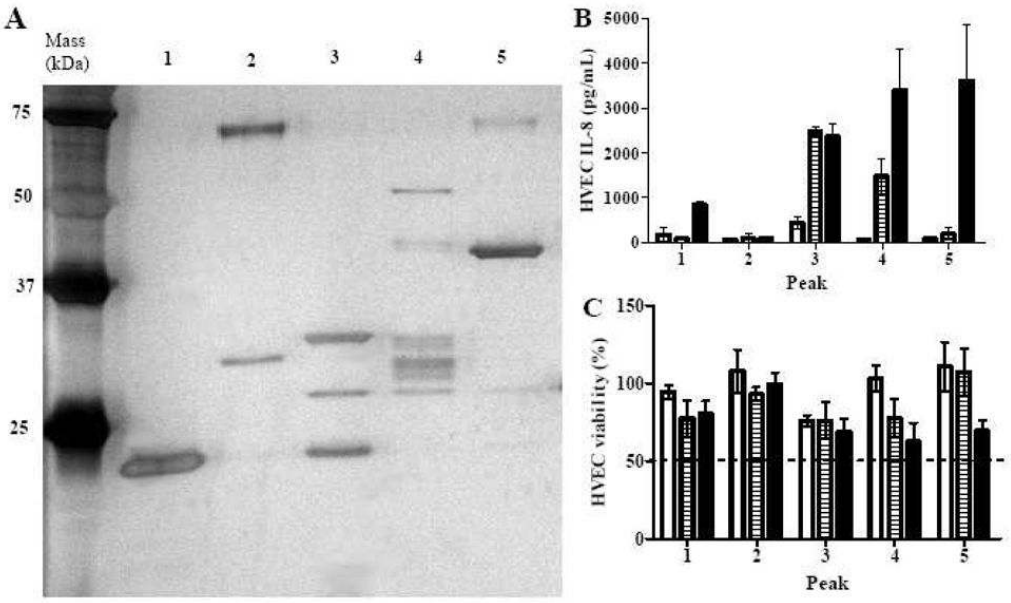

Figure 6. Proteins and biological activities of CDC587 rHPLC peaks from pH 7–9 IEF fractions

(A) Peaks from rHPLC (approximately 250 ng) separated by 12% SDS-PAGE. Proteins on the gel were identified according to molecular mass and mass spectrometry of the rHPLC peaks (Tables 1 and 2). (B) IL-8 production by HVECs treated with CDC587 rHPLC peaks. (C) Viability of HVECs treated with CDC587 rHPLC peaks. (open bar, 0.2 μg/ml; gray bar, 2 μg/ml; closed bar, 20 μg/ml). The data were presented as mean ± range of the duplicates.

NIH-PA Author Manuscript

NIH-PA Author Manuscript

NIH-PA Author Manuscript

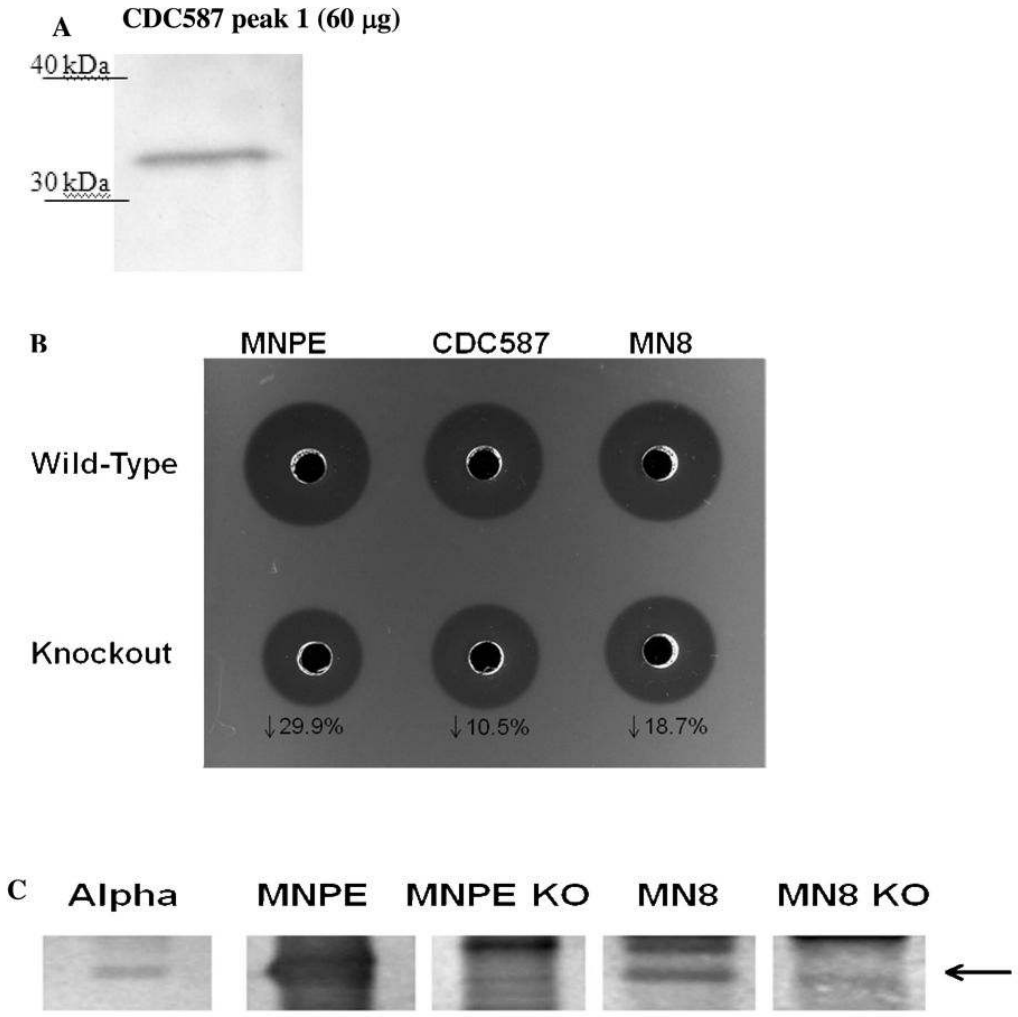

Figure 7. Evidence of functional αα α-toxin production by CDC587

(A) Western blot of 60 μg of CDC587 peak 1 from rHPLC with anti-α-toxin monoclonal antibody (MAb). (B) Hemolysis of rabbit red blood cells by 5μl of supernatants obtained from sterile filtered, overnight cultures of TSS^+ *S. aureus* wild-type MNPE, CDC587, MN8 and corresponding KO strains. (C) Western blot of 5μl of supernatants from sterile filtered, overnight cultures of TSS^+ *S. aureus* wild-type MNPE, MN8 and corresponding KO strains. α–toxin (purified from MNPE by isoelectric focusing and rHPLC, 0.5μg) was used as a positive control.

NIH-PA Author Manuscript

NIH-PA Author Manuscript

NIH-PA Author Manuscript

Table 1

Virulence factors recovered from *S. aureus* MNPE

Protein (gene)	Accession (GI version)	MW (kDa)	pI
Staphylococcal complement inhibitor (*scn*)	88195845	13,052	9.3
Staphylokinase precursor (*sak*)	49484186	18,474	6.8
Thermonuclease precursor (*nuc*)	88194577	25,120	9.3
Toxic shock syndrome toxin-1 (*tst*)	15927587	26,447	8.8
Enterotoxin type C3 (*sec3*)	15927585	30,671	8.2
α-toxin precursor (*hla*)	15926746	35,975	8.7
Staphopain A (*scpA*)	49484150	44,048	9.6
Trypsin-like serine protease	82751315	45,764	9.2
Lipase (*lip*)	88196625	76,675	7.1

NIH-PA Author Manuscript

NIH-PA Author Manuscript

NIH-PA Author Manuscript

Table 2

Virulence factors recovered from CDC587

Protein (gene)	Accession (GI version)	MW (kDa)	pI
Antimicrobial protein; Phenol soluble modulin β1	49483337	4,496	4.8
Staphylococcal complement inhibitor (*scn*)	88195845	13,052	9.3
Staphylococcal accessory regulator A (*sarA*)	88194390	14,718	7.8
MHC class II analog protein	88194675	15,838	9.3
Chemotaxis inhibitory protein (*chp*)	88195846	17,040	9.6
Staphylokinase precursor (*sak*)	49484186	18,474	6.8
Signal transduction protein TRAP (*traP*)	49484076	19,601	6.2
Thermonuclease precursor (*nuc*)	88194577	25,120	9.3
Exotoxin 1, Superantigen family protein 7, (*set1*)	49482656	26,051	6.9
Superantigen-like protein	49482662	26,378	8.7
Toxic shock syndrome toxin-1 (*tst*)	15927587	26,447	8.8
Secretory antigen SsaA-like protein	88194436	28,187	6.1
Staphylococcal enterotoxin type C (*sec*)	15927585	30,671	8.2
γ-toxin component A (*hlgA*)	49484635	34,958	9.6
γ-toxin component C (*hlgC*)	49484636	35,642	9.3
α-toxin precursor (*hla*)	15926746	35,975	8.7
γ-toxin component B (*hlgB*)	49484637	36,812	9.3
1-Phosphatidylinositol phosphodiesterase (*plc*)	49482345	37,114	7.1
Staphopain A (*scpA*)	49484150	44,048	9.6
Iron-regulated binding protein (*isdB*)	49483291	72,999	9.0
Lipase precursor (*lip1*)	49484866	76,601	7.8
Lipase precursor (*lip2*)	49482552	76,691	9.0
5′-Nucleotidase (*sasH*)	49482276	85,133	9.2
Fibronectin-binding protein precursor (*fnbA*)	49484704	105,691	4.6